JVSTB
JOURNAL OF VACUUM SCIENCE AND TECHNOLOGY B

Transport behavior of atomic layer deposition precursors through polymer masking layers: Influence on area selective atomic layer deposition

Ashwini Sinha, Dennis W. Hess, and Clifford L. Henderson

Citation: J. Vac. Sci. Technol. B **25**, 1721 (2007); doi: 10.1116/1.2782546
View online: http://dx.doi.org/10.1116/1.2782546
View Table of Contents: http://avspublications.org/resource/1/JVTBD9/v25/i5
Published by the AVS: Science & Technology of Materials, Interfaces, and Processing

Transport behavior of atomic layer deposition precursors through polymer masking layers: Influence on area selective atomic layer deposition

Ashwini Sinha, Dennis W. Hess, and Clifford L. Henderson[a)]
School of Chemical and Biomolecular Engineering, Georgia Institute of Technology, 311 Ferst Drive NW, Atlanta, Georgia 30332-0100

(Received 13 June 2007; accepted 20 August 2007; published 21 September 2007)

Sorption and diffusion of precursors through polymer layers were considered as limitations to the successful implementation of a polymer film-based masking approach to area selective atomic layer deposition techniques (ASALDT). Quartz crystal microbalance studies were used to estimate solubility and diffusivity of ALD precursors through supported thin polymer films at elevated temperatures. Specifically, measurements have been performed to estimate the solubility of water in polyhydroxystyrene, polymethylmethacrylate (PMMA), and hexafluoroisopropylalcohol polynorbornene. In addition, diffusion coefficients and solubilities of titanium tetrachloride ($TiCl_4$) and titanium isopropoxide [$Ti(ipr)_4$] through PMMA have also been determined. The results suggest that polymer films exhibit insignificant water uptake at high temperature ($\sim$160 °C) and, hence, sorption of water into polymer films does not pose limitations to polymer masking-based ASALDT. Diffusion coefficient measurements of metal precursors account for the role of precursor size in determining the minimum polymer masking layer thickness for a successful ASALDT process. [DOI: 10.1116/1.2782546]

I. INTRODUCTION

Area selective atomic layer deposition techniques (ASALDT) have been successfully implemented to perform direct patterned deposition of a variety of metal oxide thin films such as HfO_2, ZnO, TiO_2, and ZrO_2. All initial approaches on developing ASALDT invoked self-assembled monolayers (SAMs) of octadecyltrichlorosilane to chemically passivate the active reaction sites on the growth surface and, thus, block ALD nucleation.[1–4] Previous studies demonstrated that it is essential to obtain a defect-free monolayer in order to avoid nucleation in undesired locations.[5,6] Unlike SAMs, polymers can be quickly and easily spin coated to obtain defect-free thin films. Indeed, we have previously utilized this advantage of polymer films to develop a polymer-based masking approach to ASALDT.[5,7] However, it is important to note that, unlike previous efforts in which SAMs were used to passivate reactive surface functional groups by chemical reaction with the SAM, polymer films do not, in general, directly react with the substrate surface. Instead, the polymer simply physically coats the surface and serves as a diffusion barrier that physically blocks the reactive substrate surface groups from ALD precursors. While this permits the polymer films to be easily coated and easily removed from the surface after deposition, it also means that reactive surface functional groups still exist at the bottom of the protective polymer masking layer. Therefore, although the polymer film is designed to be unreactive towards the ALD precursors, if the ALD precursor has sufficient time to diffuse through the polymer film and reach the underlying substrate, they will react with surface species and nucleate growth of the ALD material beneath the polymer film.

This submasking layer growth phenomenon was demonstrated in previous publications.[5,7] During the course of those investigations, it was observed that precursor sorption and diffusion through polymer masks play critical roles in establishing a controllable and robust ASALDT process based on polymer masks. In particular, the diffusion coefficient of metal precursors controlled the masking layer thickness required, and equilibrium uptake of the precursors in combination with the diffusion coefficient directly determine the remnant precursor concentration after each ALD half-cycle. If the reaction chamber is not adequately purged, these remnant precursors can serve as nucleation sites in the masking film and cause failure of the ASALDT process. In this article, we investigate the transport properties of ALD precursors through the polymer films investigated in our previous studies. Specifically, sorption of water in different polymers that could form the basis of lithographically definable masking layers, including polyhydroxystyrene (PHOST), hexafluoroisopropylalcohol (HFA-PNB), and polymethylmetacrylate (PMMA), at different temperatures has been investigated. The results presented in this study address whether sorption of water into polymer films poses limitations for the implementation of polymer masking layers for ASALDT processes. In a similar manner, the measured transport properties of metal precursors through these same polymers will generate insight into the observed critical dependence of the required masking layer thicknesses on metal precursor choice.

II. EXPERIMENT

A. Experimental apparatus

A schematic of the experimental apparatus used for sorption studies is presented in Fig. 1. The apparatus consisted of

[a)]Author to whom correspondence should be addressed; electronic mail: cliff.henderson@chbe.gatech.edu

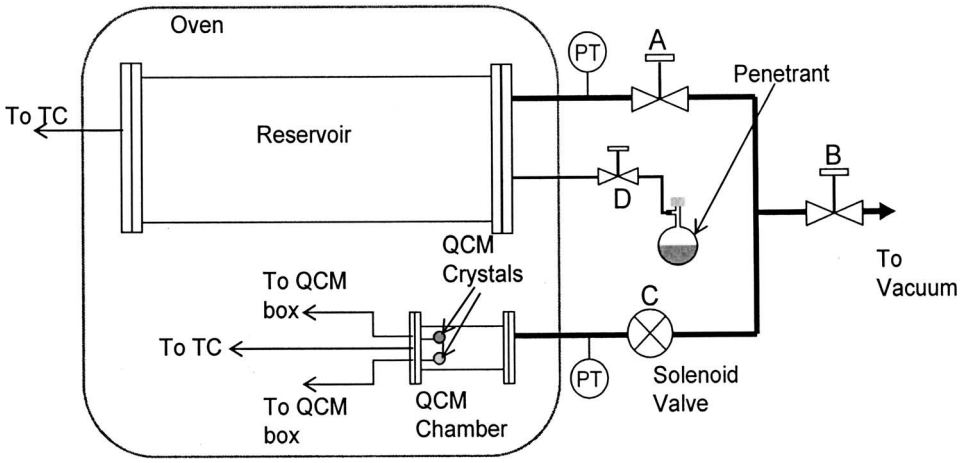

FIG. 1. Schematic of the QCM sorption/desorption apparatus used in this work.

two different size chambers placed inside a mechanical convection oven (Yamato Scientific, DKN 600 series). The smaller chamber housed two quartz crystal microbalance (QCM) crystals, while the larger chamber served as a gas reservoir. The pressure in both chambers was monitored using Barocel 622 series pressure transducers with bakeable sensor heads. The sensor heads can be heated to 200 °C and offer reliable measurements independent of vapor phase composition when operated within this temperature limit. However, the zero reading for the pressure transducer connected to the larger chamber shifted by 0.13–0.14 Torr when heated above 60 °C, thereby causing a fixed offset of 0.13–0.14 Torr in the pressure readings. The transducer connected to the smaller chamber delivered stable pressure measurements at all temperatures. Temperature measurements were performed using a *K*-type thermocouple (TC) (Omega Inc.) with a stainless steel (SS) sheath and grounded junction. The SS sheath protected the TC junction from corrosive environments (e.g., $TiCl_4$), and the grounded junction type was chosen for its rapid response relative to that of an ungrounded junction type. The penetrants used for sorption and desorption experiments were stored in a round bottom flask and were subjected to at least three freeze-pump-thaw cycles before use in order to remove noncondensable gases absorbed in the penetrant liquid.

Gold plated AT-cut quartz crystals [Anderson Electronics Inc., electrode size: 0.435 in. diameter (top) and 0.250 in. diameter (bottom)], with a nominal resonance frequency of 5 MHz in the fundamental mode, were used for QCM measurements. A crystal holder (HC-51), also obtained from Anderson Electronics Inc., was converted into a vacuum seal crystal holder for our experiments by passing the lead wire through holes drilled in a 2.75 in. Conflat blank and then sealing the holes with an epoxy sealant (Duralco 4700 series, Cotronics Corp.), which is stable for continuous operation up to 350 °C. This custom-made crystal holder allowed the use of a small QCM chamber (volume: ~55 cm^3), such that the pressure change upon opening the small chamber to the large reservoir chamber could be minimized. The crystal frequency was measured using a commercial Maxtek RQCM system, and data were logged at a frequency of 20 Hz. The entire system was maintained under vacuum using an Alcatel 2033 C2 series vacuum pump. A liquid nitrogen trap was installed upstream of the vacuum pump to prevent penetrant vapors from entering the pump.

B. Materials and sample preparation

PMMA (MW: 54 000) (MW denotes molecular weight) was obtained from Scientific Polymer; PHOST (MW:11 800) was obtained from DuPont Electronic Materials; and bis-trifluoromethyl carbinol substituted polynorbornene (i.e., HFA-PNB) (MW: 13 400) was obtained from Promerus Inc. The chemical structures of these materials are presented in Fig. 2. Toluene (99%, Aldrich) was used as the casting solvent for PMMA and propylene glycol methyl ether acetate (99%, Aldrich) was used as the casting solvent for PHOST and HFA-PNB. Polymer resins were dissolved in the respective casting solvents to prepare solutions containing 5–15 wt % of solids. Solutions were filtered through a 0.45 μm Teflon filter and spin coated onto QCM crystals using a CEE Model 100 CB spin coat and bake system to create films ranging in thickness from 400 to 1000 nm. A soft bake of 95 °C for 4 min was performed for PMMA and PHOST films, whereas HFA-PNB films were soft baked for 4 min at 105 °C to remove residual casting solvent left in the film. The films were exposed to vacuum for at least 1 h after being loaded into the QCM chamber, which further ensured that the residual solvent in the films was minimized or eliminated.

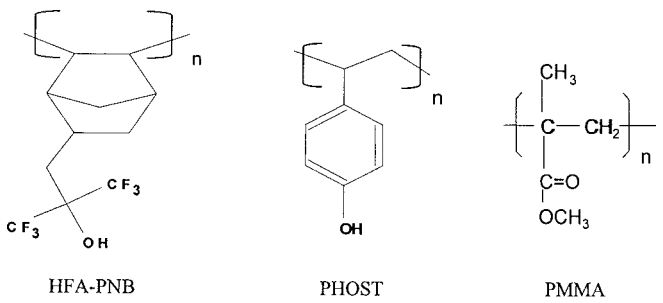

FIG. 2. Chemical structure of polymers investigated in this study.

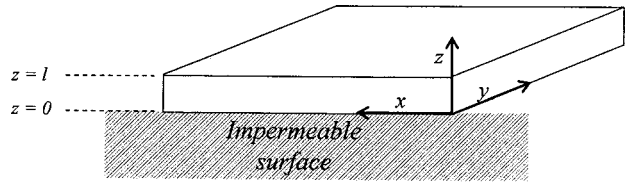

FIG. 3. Schematic of the 1D geometry used in this study.

C. Film thickness measurements

Polymer film thicknesses were measured using variable angle spectroscopic ellipsometry (M-2000 ellipsometer, J.A. Woollam Co. Inc.). Ellipsometry data were collected over the wavelength range from 400 to 1000 nm at angles of 65°, 70°, and 75° (with respect to the substrate plane normal). Data were analyzed to determine the film thickness and refractive index using the WVASE-32 software package (J.A. Woollam Co.) by fitting the ellipsometry data using a film stack model composed of a Cauchy layer model for the polymer film and a semi-infinite gold film for the substrate.

D. Sorption/desorption measurements

Two QCM crystals, one polymer coated and one blank, were loaded into the QCM chamber during each experiment. The blank crystal served as a reference and was used to record changes in frequency due to pressure and temperature fluctuations that result from pressure and temperature changes inside the QCM chamber during sorption/desorption experiments. After loading the samples, both the reservoir and QCM chambers were evacuated to a base pressure of 10 mTorr and heated to the desired temperature for sorption experiments. All flow lines were also heated to the desired temperature to eliminate the possibility of vapor condensation and cooling. After the crystal frequencies stabilized, valves B and C were closed and the reservoir was filled to a desired pressure with penetrant vapor. Vapors were allowed to equilibrate to the chamber temperature for at least 10 min and then valve C was opened. The reservoir volume is approximately 24 times the volume of QCM chamber, and thus the pressure in the smaller chamber stabilized quickly to 96% of the initial reservoir pressure due to pressure differential driven flow. Also, valve C is a solenoid operated valve with response time less than 100 ms. This configuration and mode of operation allowed a change in the vapor concentration inside the QCM chamber that approximated a step function. The sequence during penetrant desorption was (1) close valve C, (2) evacuate reservoir and all the flow lines to base pressure, and (3) open valve C. This operation quickly dropped the pressure inside the QCM chamber to initiate desorption of penetrant from the polymer film.

The polymer film sorption and desorption experiments on the QCM crystals performed in this work represent a simple one-dimensional (1D) system with one impermeable side and one side exposed to a fixed concentration of a single solute or penetrant, as shown in Fig. 3. Assuming purely Fickian transport, the total mass of penetrant inside the film at any time t can be described by Eq. (1).[8]

$$\frac{M_t}{M_\infty} = 1 - \frac{8}{\pi^2}\sum_{n=0}^{\infty}\frac{1}{(2n+1)^2}\exp\left[-\frac{(2n+1)^2\pi^2 Dt}{4l^2}\right], \quad (1)$$

where M_t is the mass uptake at time t, M_∞ is the amount absorbed at equilibrium, D is the diffusion coefficient of solute through the polymer film, and l is the film thickness. Thus, by performing sorption experiments for different penetrants in a polymer system, we can estimate the equilibrium uptake and diffusion coefficient of the penetrant through a specific polymer film.

QCM offers a convenient technique to perform sorption experiments on supported films since the frequency of oscillation of a quartz crystal decreases when mass is loaded onto the crystal surface. Sauerbrey, in 1959, demonstrated that the change in resonance frequency of the crystal is linearly proportional to the change in mass loading, as described by Eq. (2).[9]

$$\Delta f = -\frac{2f_o^2\Delta m}{A\sqrt{\mu\rho}} = -C\Delta m, \quad (2)$$

where Δf=change in frequency, f_o=fundamental resonant frequency of unloaded quartz crystal, Δm=mass change, A=surface area, μ=shear modulus of the AT-cut quartz, and ρ=density of quartz.

Hence, the M_t/M_∞ value for a given penetrant/polymer system was obtained conveniently by

$$\frac{M_t}{M_\infty} = \frac{f_t - f_{t=0}}{f_\infty - f_{t=0}}, \quad (3)$$

where f_t=frequency at time t, f_∞=stabilized frequency after sorption/desorption, and $f_{t=0}$=frequency at the start of sorption/desorption.

Equilibrium mass uptake was determined from

$$\frac{M_\infty}{M_{\text{polymer}}} = \frac{f_\infty - f_{t=0}}{f_{\text{uncoated}} - f_{\text{coated}}}, \quad (4)$$

where f_{uncoated}=frequency of crystal without polymer coating and f_{coated}=frequency of crystal after polymer film coating.

It is important to note that the Sauerbrey equation is only valid for thin films that can be considered as rigid masses.[10,11] If the film is not a rigid mass, the shear wave in the QCM crystal propagates into the coated film and looses a significant amount of energy. This energy loss will in turn affect the frequency measurement, and the crystal behavior can deviate extensively from the Sauerbrey relationship. The rigid mass requirement for the Sauerbrey equation is especially important for high mass loadings on QCM crystals. A good indicator of the elastic behavior of the quartz crystal/polymer film system is the ratio of the acoustic impedance (Z) of the respective materials. As the elastic behavior of the polymer film changes, the value of Z changes as well. It has been shown that, for high mass loadings on a QCM crystal, significant deviations from the Sauerbrey equation can occur for small changes in Z. This may result in errors in the mass

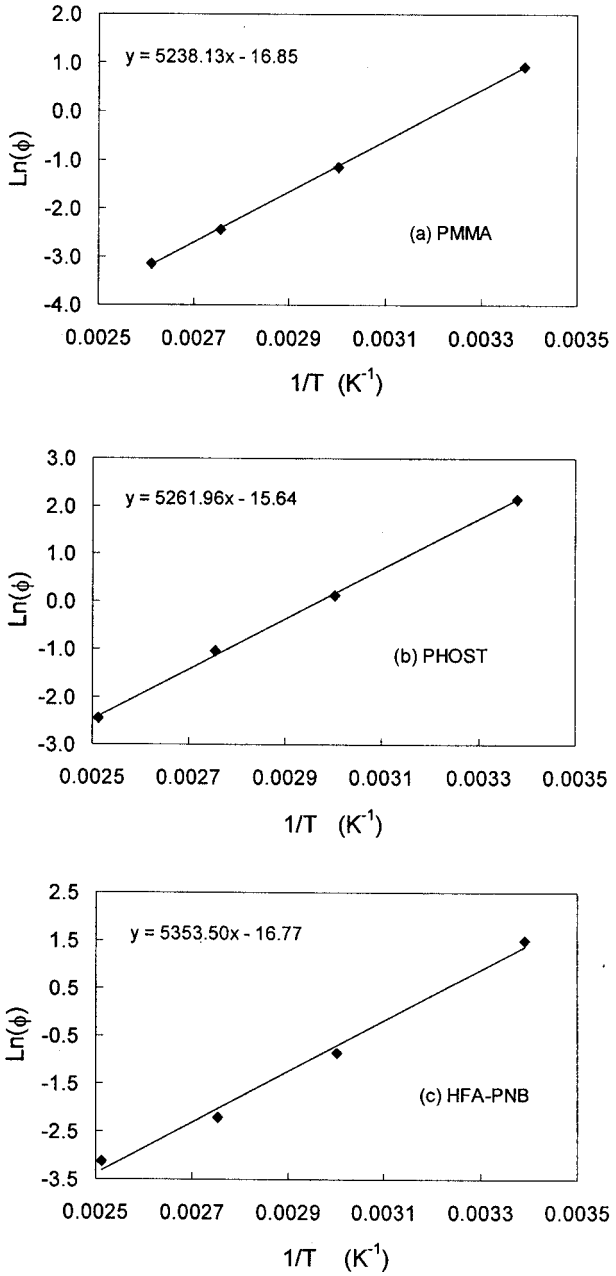

FIG. 4. Van't Hoff plots for water sorption in PMMA (a), PHOST (b), and HFA-PNB (c) films using a water vapor pressure of 20 Torr.

calculated, as penetrant is absorbed into the polymer films, if the films are plasticized sufficiently for their elastic behavior (Z value) to change significantly. Fortunately, any changes in the elastic behavior of the polymer films studied in this work were not expected to create a significant deviation from the Sauerbrey equation due to the relatively low mass uptake of the penetrant molecules. This conclusion is supported by the observation that, although a change in Z at high mass loadings creates significant measurement errors, at low mass loadings or crystal frequency shifts (i.e., delta frequency due to mass addition divided by crystal resonant frequency less than 0.05), the mass/frequency relationships for all values of Z converge on the Sauerbrey relationship.[11] The frequency shift ratios observed in the experiments reported here were very small (0.001–0.002), and thus the use of the Sauerbrey relationship to determine the mass added to the crystal from the resonance frequency shift should introduce insignificant error. In addition, dissipation factors of polymer coated crystals at all temperatures investigated were also monitored by QCM-D (Q-sense, QCM with dissipation monitor) measurements. Dissipation factor is defined as the ratio of the loss modulus to the storage modulus and, thus, is an indicator of the softness or damping ability of the film coated on the crystal. The differences in dissipation factor of uncoated and polymer coated crystals at all temperatures studied were $<6\%$, which further supports the validity of the Sauerbrey relationship for our specific studies.

TABLE I. Estimated heat of sorption of water in PHOST, HFA-PNB, and PMMA.

Polymer	Heat of sorption ($-\Delta H_s$), kJ/mol
PHOST	43.75
HFA-PNB	44.47
PMMA	43.55

III. RESULTS AND DISCUSSIONS

A. Water sorption studies

Water sorption studies were conducted on three different polymers: PMMA, PHOST, and HFA-PNB. De-ionized water, maintained at room temperature (22–23 °C), served as the source for water vapor. Transport properties of water through PMMA (Refs. 12–16) have been studied extensively; however, limited literature has been published for PHOST and HFA-PNB.[10,17,18] One of the objectives of our study was to estimate equilibrium water vapor uptake by these polymers at elevated temperatures. Figure 4 presents Van't Hoff plots for PMMA, PHOST, and HFA-PNB in the temperature range of 295–398 K, where ϕ is the percent equilibrium mass uptake of water by the polymers. The data presented are for sorption when the polymer films were exposed to a water vapor pressure of 20 Torr.

Figure 4 indicates that, at a fixed pressure, the equilibrium sorption uptake decreased monotonically with an increase in temperature; all polymers displayed an exponential increase in water sorption with $1/T$. The slopes of the lines in Fig. 4 can be used to estimate the heat of sorption of water in these polymers, and the calculated values are listed in Table I.

Interestingly, despite very different molecular structures and equilibrium water vapor uptakes, the three polymers exhibit very similar heats of sorption that are essentially the same as the heat of condensation of water (–43.5 kJ/mol), suggesting a negligible heat of mixing of water in these polymers. The equilibrium solubilities at different temperatures were also compared after normalizing the activity of water (pressure) by the water saturation vapor pressure (P_{sat}) at the corresponding temperatures. Values of water solubility at dif-

TABLE II. Estimated solubility of water vapor in PHOST, HFA-PNB, and PMMA under different experimental conditions.

Polymer	ϕ $T=295$ K, $P=20$ Torr	ϕ $T=433$ K, $P=20$ Torr	ϕ $T=433$ K, $P=0.22$ Torr	Mol H_2O/mol monomer unit $T=433$ K, $P=0.22$ Torr
PHOST	8.52	0.029	0.008 82	2.13×10^{-5}
HFA-PNB	4.52	0.011	0.000 12	1.84×10^{-5}
PMMA	2.51	0.008	0.000 086	4.76×10^{-6}

ferent temperatures collapsed into a single curve, which also confirmed a negligible heat of mixing of water in the polymers.[19]

Unfortunately, direct measurement of equilibrium moisture uptake at 433 K (160 °C) could not be performed because of very low mass uptake at that temperature which resulted in <1 Hz frequency change upon exposure to 20 Torr of water vapor. The observed change in frequency of the blank crystal due to a change in pressure was also of the same order of magnitude, making it difficult to acquire reliable data. However, the mass uptake at 160 °C can be estimated by extrapolating the Van't Hoff plots presented in Fig. 4. It should be noted that the glass transition temperature of PMMA and PHOST is ~115–120 and ~105–110 °C respectively; as a result, they are in a rubbery phase at 160 °C. Heat of sorption is generally reduced when a polymer is heated beyond its T_g; thus, the extrapolated value of equilibrium uptake could differ from the actual value.[20] Nevertheless, estimations can be obtained from the data collected; these are shown in Table II.

In addition, the actual pressure increase during the water exposure step in our ALD experiments was measured to be only 0.21–0.22 Torr. Thus, assuming that Henry's law is applicable under these conditions, the values of mass uptake have been linearly scaled to an exposure pressure of 0.22 Torr. The last column in Table II provides the estimated ratio of moles of water sorbed in the films per mole of monomer unit in the polymer chain at equilibrium with 0.22 Torr of water vapor. It is evident that all the polymers investigated in this study demonstrated very low water uptake under actual ALD conditions. Furthermore, the reported data represent the equilibrium absorbed amount; the remnant water after the purge is expected to be much lower. All the polymers investigated in this study have one active site per monomer unit (although of varying reactivity and accessibility). Therefore, the data presented in Table II clearly indicate that the increase in the number of active sites upon water sorption is minimal, indicating that most of the nucleation on these polymer films during ALD results primarily from active sites present in the polymer backbone. These results demonstrate that water sorption in masking layers is not critical and does not pose a significant limitation in the successful application of polymer-based masking approaches for ASALDT processes. This conclusion is further supported by observations reported in our previous studies where x-ray photoelectron spectroscopy analyses did not detect TiO_2 nucleation on polystyrene using $TiCl_4/H_2O$ and titanium isopropoxide $[Ti(ipr)_4]/H_2O$, and on PMMA using $Ti(ipr)_4/H_2O$ as ALD precursors.[7,21] Thus, if a polymer masking layer can be identified as unreactive towards a metal precursor, a cumbersome SAM-based masking approach can be replaced by a more convenient polymer-based masking approach. Success of such a scheme has already been documented elsewhere.[7]

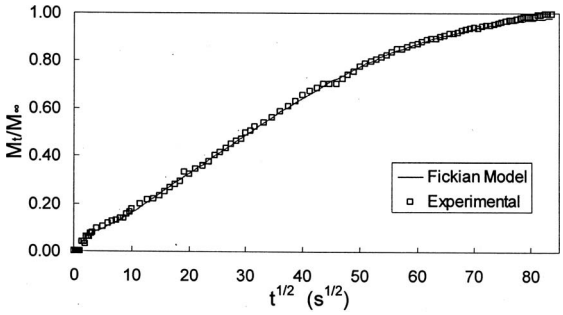

FIG. 5. Sorption curve for titanium isopropoxide in PMMA at 160 °C. $P=3.8$ Torr, film thickness=805 nm.

B. Titanium isopropoxide and titanium tetrachloride sorption studies

In order to further explore the barrier properties of polymer layers for TiO_2 ASALDT, diffusion coefficients of $Ti(ipr)_4$ and $TiCl_4$, which are two common titanium precursors used for ALD, were studied in PMMA films. Titanium isopropoxide sorption studies were conducted at an exposure pressure of 3.7–3.8 Torr, whereas $TiCl_4$ sorption was conducted at 1.4 and 9.8 Torr. Titanium isopropoxide was heated to ~85 °C to generate sufficient vapor pressure, while $TiCl_4$ was maintained at room temperature (~22–23 °C). Figure 5 is a representative sorption curve (fractional mass uptake versus square root of time) obtained at 433 K (160 °C). A Fickian diffusion coefficient has been estimated from the slope of the initial portion of the sorption curve using Eq. (5), and the Fickian diffusion relationship is then plotted using Eq. (1).

$$\frac{(M_t/M_\infty)_{t_1}-(M_t/M_\infty)_{t_2}}{\sqrt{t_1}-\sqrt{t_2}}=\frac{2}{l}\left(\frac{D}{\pi}\right)^{1/2}. \tag{5}$$

Sorption experiments were also conducted at temperatures of 125, 135, and 145 °C in order to estimate mass uptake, and the diffusion coefficient of titanium isopropoxide as a function of temperature; such information is valuable for further experimental design. The diffusion coefficient and percent equilibrium mass uptake at these temperatures are presented in Figs. 6 and 7, respectively.

Titanium isopropoxide follows Fickian sorption behavior into PMMA in the temperature range of 125–160 °C. The equilibrium mass uptake at 160 °C was 0.043 wt % of the polymer and the diffusion coefficient was estimated to be 1.35×10^{-16} m^2/s. However, an uptake of 0.043 wt % is observed when the polymer films were exposed to a vapor pressure of 3.8 Torr. In our previous area selective ALD

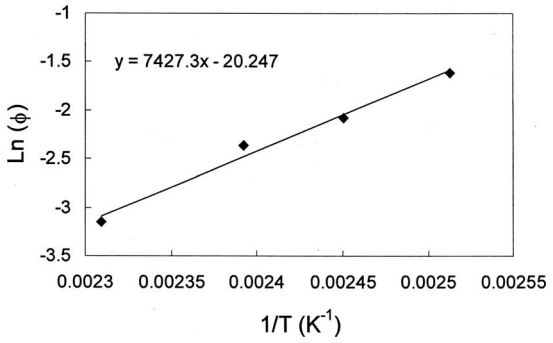

FIG. 6. Van't Hoff plot for titanium isopropoxide sorption in PMMA.

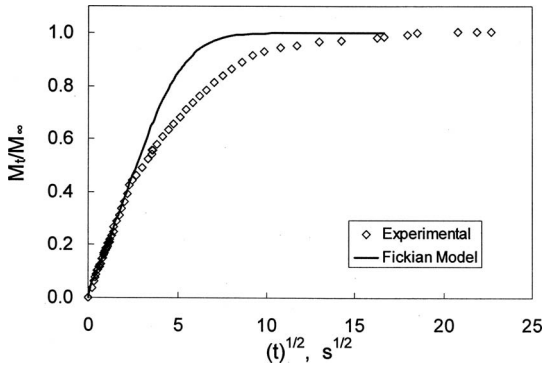

FIG. 8. Sorption kinetics of $TiCl_4$ in PMMA at 160 °C. $P=1.4$ Torr, Film thickness=748 nm.

experiments,[7] the pressure pulse observed during isopropoxide exposure for 2 s was ~0.03 Torr. Thus, analogous to the water sorption case, the actual uptake of isopropoxide during ALD experiments is estimated to be 0.000 34 wt % of the polymer.

Sorption experiments were also performed for $TiCl_4$. $TiCl_4$ exhibited significantly higher uptake in PMMA than did titanium isopropoxide at all temperatures investigated. In addition, the equilibrium uptake of $TiCl_4$ in PMMA increases with temperature. The mass uptake value (obtained from sorption experiment at 9.5 Torr) increased from ~1.1 to ~7.4 wt % as the temperature increased from 125 to 160 °C, suggesting that the overall uptake process is endothermic. As expected, $TiCl_4$ reacted with PMMA as indicated by only a partial desorption of mass originally absorbed during the sorption step. Complexation of $TiCl_4$ with carbonyl groups in PMMA added a bulky pendant group to the polymer chain. Furthermore, Ti is a six coordination site element and thus cross-linking of the polymer chains could occur if the same $TiCl_4$ molecule reacts with C=O sites from two different chains. This complexation of $TiCl_4$ with PMMA reduces the mobility of polymer chains resulting in a reduction in diffusion coefficient as $TiCl_4$ is absorbed into the polymer film. This effect is evident by the significant deviation of the sorption curve (at 1.4 Torr) from Fickian kinetics, as shown in Fig. 8.

During our previous ALD experiments,[5] PMMA was exposed to very low concentrations of $TiCl_4$ (pressure pulse of ~0.09–0.1 Torr) and, hence, the sorption kinetics data collected at an exposure pressure of 1.40 Torr (sorption kinetics presented in Figs. 8 and 9) were used to estimate the diffusion coefficient under experimental conditions more representative of actual ALD conditions. Moreover, since $TiCl_4$ reacts with PMMA, thereby changing its transport properties, the diffusion coefficient of $TiCl_4$ in unmodified PMMA is estimated by the slope of the curve where $M_t/M_\infty \rightarrow 0$, as shown in Fig. 9. The estimated diffusion coefficient is 1.53×10^{-14} m^2/s. It should be noted that, since the diffusion coefficient of $TiCl_4$ is strongly concentration dependent (decreases with an increase in concentration), the estimated diffusion coefficient based on initial time data from sorption at 1.4 Torr could still be lower than the actual diffusivity of $TiCl_4$ molecules at the lower activity (i.e., lower vapor pressure) experienced during ALD experiments. That is, although the overall penetrant uptake in the film at the start of the sorption is low, the top surface reaches instantaneous saturation. Based on the reaction time scale, the mobility of polymer chains in the film regime near the top of the layer will decrease, leading to a reduction in diffusion coefficient of the incoming penetrant or the penetrant already present. This effect will limit further transport of penetrant into the polymer film (which only occurs from the top layer) and yield slower uptake and, thus, a lower diffusion coefficient. We have estimated the diffusion coefficient from short-time data (below 1 s of sorption); in addition, the diffusivity calculated

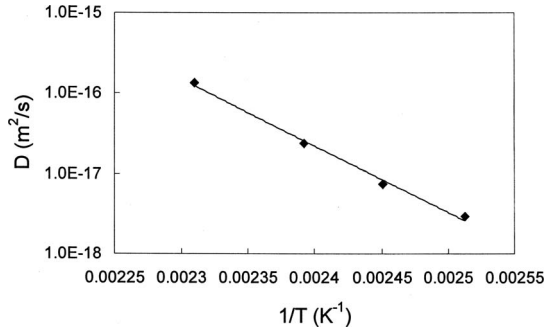

FIG. 7. Diffusion coefficient of titanium isopropoxide in PMMA at different temperatures.

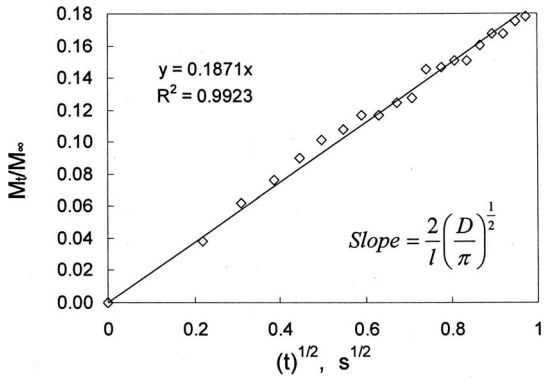

FIG. 9. Estimation of diffusion coefficient of $TiCl_4$ in PMMA at 160 °C using the initial portion of the sorption curve.

based on sorption kinetics obtained at 9.5 Torr was 1.24×10^{-14} m^2/s, which is only 20% smaller than the value obtained at 1.4 Torr. Thus, it can be concluded that the estimated diffusion coefficient based on short-time data (from sorption kinetics at 1.4 Torr) is not significantly different from the value expected at lower activity. Also, the equilibrium mass uptake at 1.4 Torr did not follow Henry's law (did not scale linearly with pressure) when compared to the equilibrium $TiCl_4$ uptake at 9.5 Torr. The equilibrium uptake at 1.4 Torr was 1.9 wt %, which is almost 70% higher than the 1.1 wt % value expected based on Henry's law. This deviation from Henry's law could be a result of changes in the polymer surface due to reaction with $TiCl_4$.

These earlier measurements suggest that the diffusion coefficient of $TiCl_4$ in PMMA is approximately two orders of magnitude higher than that for the isopropoxide precursor. These results indicate that the ratio of diffusion lengths, which scales with the square root of D, should be approximately 10. In our previous publication,[5] we noted that ~200 nm thick films were required in order to prevent nucleation at the polymer-substrate interface during $TiCl_4$–H_2O ALD. From a simple calculation of the ratio of diffusion lengths, nucleation at the interface should be observed at ~20 nm film thickness for the isopropoxide precursor system. However, the isopropoxide precursor displays much lower solubility in PMMA than does $TiCl_4$, which reduces the overall permeability and the concentration that will be observed at the polymer-substrate interface. Furthermore, with ultrathin films (25–30 nm), a greater fraction of polymer chains are confined near the substrate than will be the case with a thicker film. This confinement reduces the polymer chain mobility and is manifested in a lower diffusion coefficient in this thickness regime.[17,22] These two phenomena partially explain why no nucleation was observed for film thickness as small as 10 nm in the case of titanium isopropoxide-H_2O ALD.[7] In addition, the absolute value of average diffusion length for both precursors can be estimated by evaluating $(Dt)^{1/2}$. For an exposure time of 2 s, this value is 175 and 16 nm for $TiCl_4$ and titanium isopropoxide, respectively. The estimated values are reasonably consistent with the required masking layer thickness for both systems.

In addition to the importance of controlling the minimum required thickness of a masking layer for successful ASALDT processes, the precursor diffusion coefficient can be important from another perspective. It is beneficial to use a precursor with a low diffusion coefficient because this permits the use of a thinner masking layer. However, lower diffusion coefficients also imply that the precursor will desorb at a lower rate during the purge step. If insufficient purge duration is used, the precursor will slowly build up inside the polymer film during subsequent ALD cycles. To assess this possibility, concentration profiles of precursor inside the polymer films were evaluated by solving the 1D diffusion equation and using a diffusion coefficient of 1.35×10^{-16} m^2/s and exposure and purge times of 2 and 60 s, respectively. After only 150 cycles, a concentration of up to 3% of the equilibrium value could accumulate inside the polymer film. Under the operating conditions of our ALD experiments, titanium isopropoxide exhibits very low equilibrium uptake in PMMA. A concentration of 3% of the equilibrium uptake translates to an absolute value of 1.02×10^{-5} wt. % of titanium isopropoxide in the polymer film. Therefore, since the isopropoxide precursor does not react with the polymer and equilibrium uptake of water is low, undetectable nucleation was observed in our experiments. However, for a polymer-precursor system that exhibits a higher level of precursor solubility in the polymer film, a low diffusion coefficient of the precursor molecule can be undesirable since this would require a longer duration purge step to ensure adequate removal of penetrant from the film. This implies that, in addition to the diffusion coefficient, the solubility of the precursor in the polymer film is also an important parameter to consider in designing a successful ASALDT process.

IV. CONCLUSIONS

Sorption studies of $TiCl_4$, titanium isopropoxide, and water in polymer films using a quartz crystal microbalance technique were performed to estimate diffusion coefficients and equilibrium uptake of these ALD precursors in several polymer films. Under the operating conditions of our previous ALD experiments,[5,7,21] the solubilities of water vapor in the polymer films investigated are extremely low ($\sim 10^{-4}$–10^{-5} wt % of polymer). The estimated uptake indicates that the sorption of water vapor in polymer masking layers is not a significant issue and, hence, does not pose limitations on the implementation of polymer-based masking approaches for ASALDT. In fact, the sorption and transport properties of metal precursors played a greater role in determining the specific parameters needed for area selective ALD processes. Estimation of diffusion coefficient data for titanium isopropoxide and titanium tetrachloride in PMMA helped explain the differences observed previously in the masking layer thicknesses required for successful ASALDT of TiO_2. Transport studies have indicated that, although the use of precursors with lower diffusion coefficients in the polymer films allows the use of thinner masking layers for successful processes, such situations also demand longer purge times for complete removal of precursor sorbed during the exposure step. As a result, optimization of polymer/precursor combinations will be needed during ASALDT process development.

ACKNOWLEDGMENTS

The authors would like to gratefully acknowledge Applied Materials for their support of this work through a graduate fellowship to one of the authors (A.S.).

[1] R. Chen, H. Kim, P. C. McIntyre, D. W. Porter, and S. F. Bent, Appl. Phys. Lett. **86**, 191910 (2005).
[2] M. Yan, Y. Koide, J. R. Babcock, P. R. Markworth, J. A. Belot, T. J. Marks, and R. P. H. Chang, Appl. Phys. Lett. **79**, 1709 (2001).
[3] K. J. Park, J. M. Doub, T. Gougousi, and G. N. Parsons, Appl. Phys. Lett. **86**, 051903 (2005).
[4] M. H. Park, Y. J. Jang, H. M. Sung-Suh, and M. M. Sung, Langmuir **20**,

2257 (2004).
[5]A. Sinha, D. W. Hess, and C. L. Henderson, J. Electrochem. Soc. **153**, G465 (2006).
[6]R. Chen, H. Kim, P. C. McIntyre, and S. F. Bent, Appl. Phys. Lett. **84**, 4017 (2004).
[7]A. Sinha, D. W. Hess, and C. L. Henderson, J. Vac. Sci. Technol. B **24**, 2523 (2006).
[8]J. Crank, *The Mathematics of Diffusion*, 2nd ed. (Oxford University Press, Oxford, 1975), p. 414.
[9]G. Sauerbrey, Z. Phys. **155**, 206 (1959).
[10]C. M. Berger and C. L. Henderson, Polymer **44**, 2101 (2003).
[11]C. Lu and A. W. Czanderna, *Applications of Piezoelectric Quartz Crystal Microbalances* (Elsevier, New York, 1984), Vol. 7, p. 393.
[12]J. A. Barrie and D. Machin, Trans. Faraday Soc. **67**, 244 (1971).
[13]F. Bueche, J. Polym. Sci. **14**, 414 (1954).
[14]P. P. Roussis, J. Membr. Sci. **15**, 141 (1983).
[15]L. S. A. Smith and V. Schmitz, Polymer **29**, 1871 (1988).
[16]J. A. Barrie and D. Machin, Trans. Faraday Soc. **67**, 2970 (1971).
[17]L. Singh, Ph.D. thesis, Georgia Institute of Technology, 2004.
[18]B. D. Vogt, C. L. Soles, R. L. Jones, C. Y. Wang, E. K. Lin, W. L. Wu, S. K. Satija, D. L. Goldfarb, and M. Angelopoulos, Langmuir **20**, 5285 (2004).
[19]V. Stannett, M. Haider, W. J. Koros, and H. B. Hopfenberg, Polym. Eng. Sci. **20**, 300 (1980).
[20]W. J. Koros and M. W. Hellums, *Encyclopedia of Polymer Science and Engineering*, 2nd ed. (Wiley, New York, 1990), Supplementary Volume, pp. 724–802.
[21]A. Sinha, D. W. Hess, and C. L. Henderson, Proc. SPIE **5753**, 476 (2005).
[22]L. Singh, P. J. Ludovice, and C. L. Henderson, Proc. SPIE **5376**, 369 (2004).